ACS Sustainable Chemistry & Engineering

pubs.acs.org/journal/ascecg

Research Article

Finding a Needle in a Haystack: Producing Antimicrobial Cutin-Derived Oligomers from Tomato Pomace

Rita Escórcio, Artur Bento, Ana S. Tomé, Vanessa G. Correia, Rúben Rodrigues, Carlos J. S. Moreira, Didier Marion, Bénédicte Bakan, and Cristina Silva Pereira*

Cite This: *ACS Sustainable Chem. Eng.* 2022, 10, 11415−11427

Read Online

ACCESS | Metrics & More | Article Recommendations | Supporting Information

ABSTRACT: Agro-industrial residues comprise a rich diversity of plant polymers and bioactive compounds, constituting promising sources for the development of materials, including bioplastics, and food supplements, among other applications. In particular, the polyester cutin is abundant in fruit peel, a plentiful constituent of pomace agro-industrial residues. The potential of diverse fruit pomaces as a source for the development of cutin-derived materials/products has been extensively sought out. This study expands the established knowledge: it sets proof of concept for the production of antimicrobial oligomers from cutin-rich materials isolated in a single step from tomato pomaces generated by two remote agro-industries. Specifically, it first analyzed how the chemical signature (nuclear magnetic resonance (NMR) and gas chromatography−mass spectrometry (GC−MS)) of a pomace (and of its major constituents) mirrors that of the corresponding cutin-rich material isolated using an ionic liquid extractant. The cutin-rich materials were then deconstructed (using mild hydrolyses), and the resultant mixtures were chemically characterized and screened for bactericidal activity against *Escherichia coli* and *Staphylococcus aureus*. The presence of esterified structures, linear and/or branched, likely comprising dioic acids as a major building block (but not exclusively) is a prerequisite for activity against *E. coli* but not against *S. aureus* that was susceptible to monomers as well. Further studies are required to optimize the production of broad bactericidal oligomers from any cutin-rich pomace source, moving ahead toward their circular usage.

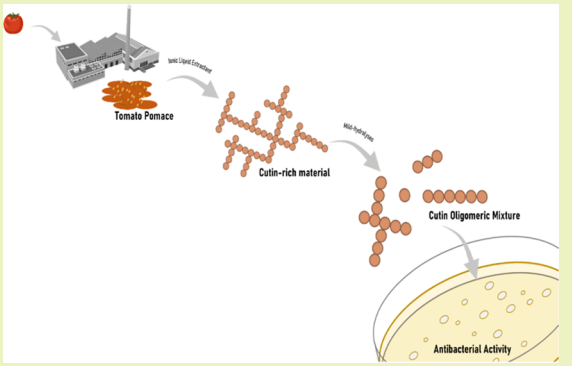

KEYWORDS: *biopolyester, cutin, pomace, antimicrobial activity, sustainable process*

INTRODUCTION

In the last decades, the environmental impact of plastics has escalated dramatically, especially as durable petroleum-based materials have been replaced by single-use products.[1,2] The development of eco-friendly alternatives for the production of materials is urgent.[2,3] The plant polyester cutin is highly abundant in nature and is considered a promising substitute for petroleum-based plastics,[4] specifically for the development of biomaterials.[5] Cutin is the major structural component of the cuticle—the outermost barrier covering the aerial parts of most land plants, where it is found embedded in waxes. The cuticle acts as an interface between the plant and the environment, contributing to limiting water loss, mechanical injury, pathogen invasion, as well as protecting against UV radiation and controlling gas exchange.[6−12] Cutin consists mostly of C_{16} and/or C_{18} ω-hydroxy acids generally functionalized with midchain hydroxyl groups, with residual amounts of glycerol, phenolics, and aromatics.[4,6,7,9,11]

In 2020, Europe processed ca. 9.8 million tons of tomato fruit, which generated ca. 0.49 million tons of pomace residue.[13,14] Portugal is the third largest processer in Europe,[14] where the derived pomace residue is mainly channeled for animal feeding. Tomato pomace consists of stems, seeds, and peels, fractions existing at variable amounts due to fruit variability and fractioning process.[15] Each fraction increases the chemical complexity of the pomace: stems mostly consist of lignin, hemicellulose, and cellulose;[15] seeds comprise diverse fatty acids (including triglycerides), polysaccharides, and proteins, having also minor amounts of suberin (found in the seed coating);[15,16] and peels contain cutin, sugars, and waxes.[4,15,17] Significantly, the tomato fruit, *Solanum lycopersicum*, is also a key plant model for cuticle and cutin studies, due to an astomatous cuticle (without cutan, an insoluble and saponification-resistant polymer) that can be easily recovered.[8,18]

Due to its easy recovery and readily availability, many studies have reported the potential use of tomato pomace as a

Received: June 14, 2022
Revised: July 22, 2022
Published: August 5, 2022

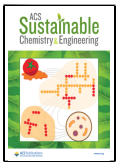

source of cutin to build structural materials.[4,15,19,20] Often these studies rely on extensive hydrolysis of the pomace for the release of fatty-based monomers (i.e., C_{16} and/or C_{18} ω-hydroxy acids), followed by their repolymerization to build a cutin-like material.[4,15,20,21] To what extent can these repolymerized materials reproduce both the native polymeric arrangement of cutin and the native barrier properties, remains seldom understood. Recent advances have however demonstrated the capacity to tune the materials' properties through poly-condensation with glycerol.[17] Finally, large-scale implementation of added value chains for tomato pomace remains challenging due to the number of processing steps, resulting in a time-consuming system.[4]

Cutin, can however, be isolated from tomato peel using a one-pot reaction with an ionic liquid extractant;[22] this method is simpler and faster compared to those frequently used to isolate cutin that combine enzymatic digestion of polysaccharides with organic solvent removal of waxes.[4,15,23−27] The extractant cholinium hexanoate preserves cutin esterification, while it washes out efficiently polysaccharides and soluble components of the cuticle (e.g., waxes), resulting in the isolation of an insoluble cutin continuum.[22,28] Studies on a related plant polyester—suberin—showed that particles can be obtained through a catalysis that partially preserves its esterified network. These particles display per se antimicrobial activity[29] and can spontaneously self-assemble forming antimicrobial films,[30] contrarily to the composing monomeric hydrolysates that do not. It is therefore hypothesized that the cutin continuum obtained with the ionic liquid-based process can be seen as a source for antimicrobial oligomers.

This study establishes knowledge grounds for the production of antimicrobial cutin oligomers through a mild deconstruction of cutin-rich materials, which were directly obtained from untreated tomato pomaces using an ionic liquid extractant. To guide discovery, nuclear magnetic resonance (NMR) and gas chromatography−mass spectrometry (GC−MS) methods were combined with bactericidal testing of the mixtures against two model bacteria: *Escherichia coli* and *Staphylococcus aureus*. How the pomace compositional signature impacts downstream the production of bioactive oligomers is discussed in great detail. The large-scale processing and extraction of cutin-rich materials from raw pomace may support the creation of novel value chains for the development of antimicrobial ingredients contributing toward a circular economy.

MATERIALS AND METHODS

Chemicals. Sodium hydroxide (>98%) from José Manuel Gomes dos Santos; methanol (≥99.8%), dimethyl sulfoxide (DMSO, >99.99%), hexane (>95%), chloroform (>99.98%), dichloromethane (>99.99%) from Fisher Chemical; cholinium hydrogen carbonate (~80% in water), hexanoic acid (>99.5%), hydrochloric acid (37%), sodium methoxide (95%), anhydrous methanol (99.8%), *N,O*-bis(trimethylsilyl)trifluoroacetamide (≥99%), pyridine (≥99.8%), heptadecanoic acid (≥98%), hexadecanedioic acid (96%), and benzoic acid (99%) from Sigma-Aldrich. Deuterated dimethyl sulfoxide-d_6 (DMSO-d_6, >99.99%) from Merck. Cholinium hexanoate was synthesized by dropwise addition of hexanoic acid to aqueous cholinium hydrogen carbonate in equimolar quantities, as previously described.[31] Purity and water level were determined as shown before.[22]

Plant Material. Tomato pomace was obtained from Sumol + Compal (Coruche, Portugal) and from the "Conserveries de Bergerac" (UNIPROLEDI, Bergerac, France). Both industrial pomaces were dried until constant weight (ca. 1 week at 60 °C). In addition, peel- and seed-rich fractions were isolated from one pomace by decantation in a water tank as previously described.[17] The floating peel-rich fraction was recovered, water excess was squeezed out by manual press and then dried at room temperature; the precipitated seed-rich fraction was freeze-dried. A stem-rich fraction was prepared by manually separating the stem fragments from the pomace. The fractions will be labeled simply as peel, seed, and stem fractions. The dried pomaces and the corresponding fractions were milled using a Retsch ZM200 electric grinder (granulometry 0.5 mm; 10000 rpm) and stored at room temperature. Pomaces were randomly designated as POM^{I-II} and POM^{III-IV}

Preparation of Cutin-Rich Materials. Cutin-rich materials were extracted from the sources as previously described.[22] The pomace and cholinium hexanoate were mixed (1:10) and stirred for 2 h at 100 °C. The reaction was stopped by the addition of DMSO 80 mL per g of cutin. The polymer was recovered by filtration using a nylon membrane filter (0.45 μm) and then filtered again while washed with an excess of deionized water. The samples were lyophilized (Labconco, −100 °C, 0.008 mbar) and stored at room temperature.

Production of Cutin Oligomeric Mixtures (COMs) through Mild Hydrolyses. *Sodium Methoxide-Catalyzed Methanolysis.* The methanolysis occurred by mixing 20 mL of anhydrous methanol in 0.1 M sodium methoxide with 0.5 g of cutin-rich material for 2 h at 40 °C without stirring. Each mixture was cooled to room temperature and centrifuged (4 °C, 30 min, 4000*g*) to obtain the nonhydrolyzed cutin fraction (pellet). The supernatant was acidified to pH 3−3.5 with HCl 37% and centrifuged (4 °C, 30 min, 4000*g*). The precipitate (^{P}) was recovered, and the supernatant was extracted three times by dichloromethane/water partition to obtain the soluble hydrolysates (^{S}); sodium sulfate anhydrous was added to remove traces of water. The organic phase was concentrated under a nitrogen flux and stored at room temperature, for further analysis. The samples were labeled as Cutin Oligomeric Mixture (COM): $COM1^P$/$COM1^S$ and $COM3^P$/$COM3^S$, where the numbers match the pomace source.

Sodium Hydroxide-Catalyzed Hydrolysis. The hydrolysis occurred by mixing 0.5 g of cutin-rich material actions with 20 mL of solution of 1 M NaOH in methanol/water (1:1, v/v) at 90 °C for 1 h without stirring. The subsequent steps were performed as previously described in sodium methoxide-catalyzed methanolysis. The samples were labeled as $COM2^P$/$COM2^S$ and $COM4^P$/$COM4^S$, where the numbers match the pomace source.

Cryogenic Grinding Process. Samples of the pomaces (including fractions) and of the extracted cutin-rich materials were cryogenically milled as described before (RESTCH Cryomill equipped with two 5 mL grinding jars of stainless steel with two 4 mm stainless steel grinding balls).[22] This step is critical for their solubilization in DMSO-d_6.

Nuclear Magnetic Resonance (NMR) Analyses. NMR spectra of pomaces (cryomilled), cutin-rich materials (cryomilled), and COMs were recorded using an Avance III 800 MHz CRYO (Bruker Biospin, Rheinstetten, Germany). All NMR spectra (^{1}H, ^{1}H−^{1}H COSY, ^{1}H−^{13}C HSQC, ^{1}H−^{13}C HMBC) were acquired in DMSO-d_6 using 5 mm diameter NMR tubes, at 60 °C as follows: 15 mg of each sample in 400 μL of DMSO-d_6. Quantitative ^{31}P NMR of the COMs was also performed using an Avance III 500 (Bruker Biospin, Rheinstetten, Germany).[32] MestReNova, Version 11.04-18998 (Mestrelab Research, S.L.) was used to process the acquired raw data. All samples were analyzed in biological triplicate (15 mg each).

Gas Chromatography−Mass Spectrometry (GC−MS). To quantify the amount of free and hydrolyzable monomers composing each COM an Agilent GC (7820A) equipped with an Agilent (5977B) MS (quadrupole) was used. The same process was used to analyze the hydrolyzable monomers in either cutin-rich material. Samples were derivatized (see below) directly or after alkaline hydrolysis (0.5 M NaOH in methanol/water (1:1, v/v), 95 °C, for 4 h; cooled to room temperature and acidified to pH 3/3.5 with 1 M HCl (37%), then extracted three times with dichloromethane/water partition). For derivatization *N,O*-bis(trimethylsilyl)-trifluoroacetamide containing 1% of trimethylchlorosilane in pyridine

https://doi.org/10.1021/acssuschemeng.2c03437
ACS Sustainable Chem. Eng. 2022, 10, 11415−11427

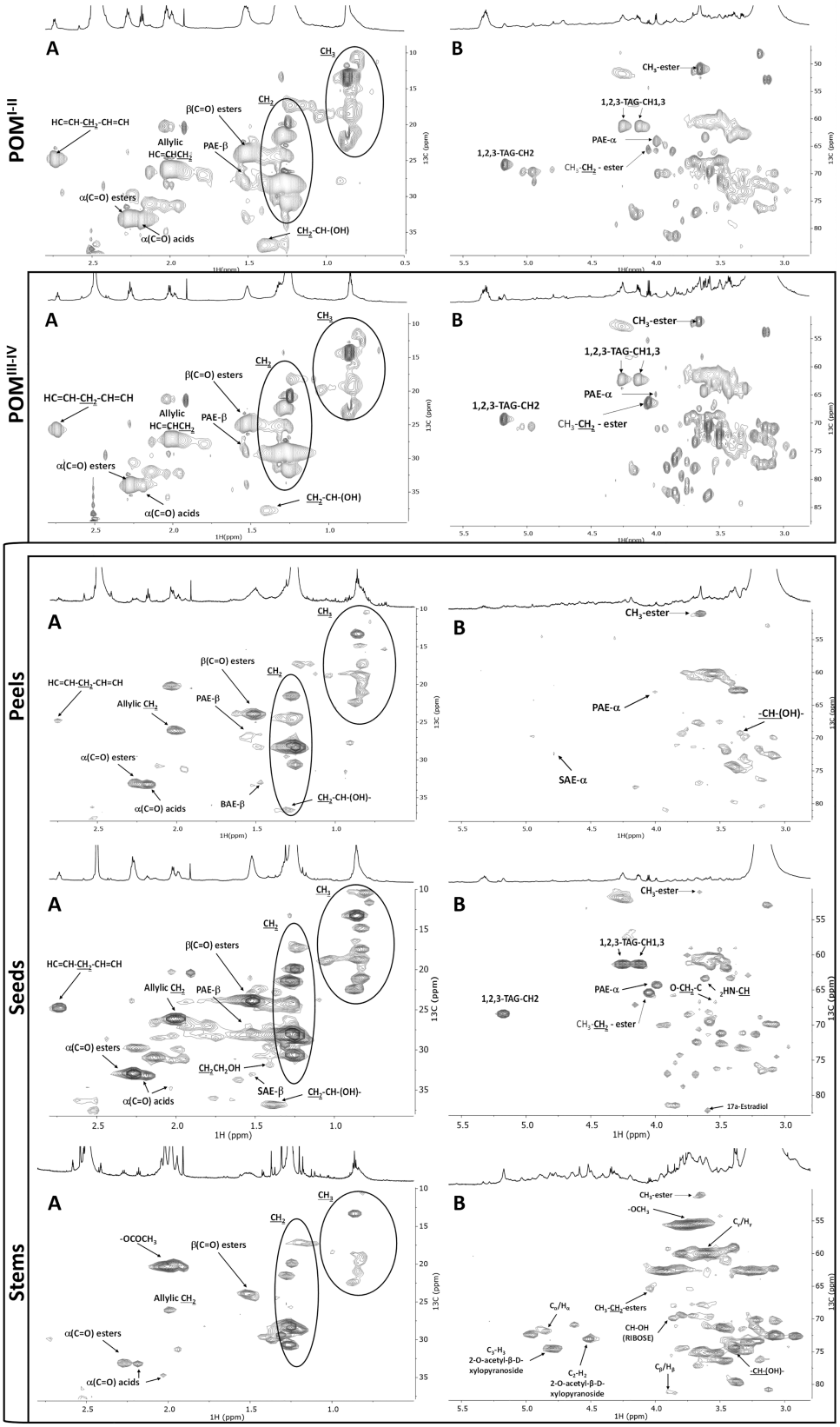

Figure 1. NMR spectral characterization of either pomace and of its composing fractions: peels, seeds, and stems. HSQC spectral characterization of each POM (top panels) and of POM$^{III–IV}$ constituents: peels, seeds, and stems (bottom panels), differentiating the aliphatic (A) and glycerol CH-acyl (B) regions. SAEs and LAEs stand for secondary and primary aliphatic esters, respectively; TAG stands for triacylglycerol. Some assignments (unlabeled) are uncertain or unidentified.

https://doi.org/10.1021/acssuschemeng.2c03437
ACS Sustainable Chem. Eng. 2022, 10, 11415−11427

(5:1) was used (30 min, 90 °C). The ensuing samples were analyzed by GC−MS (HP-5MS column) with the following ramp temperature: 80 °C, 2 °C/min until 310 °C for 15 min. MS scan mode, with a source at 230 °C and electron impact ionization (EI+, 70 eV), was used for all samples. The GC−MS was first calibrated with pure reference compounds (heptadecanoic acid, hexadecanedioic acid, and benzoic acid) relative to hexadecane (internal standard). Triplicates, each with technical triplicates were analyzed. Data acquisition was accomplished by MSD ChemStation (Agilent Technologies); compounds were identified based on the equipment spectral library (Wiley-NIST) and references relying on diagnostic ions distinctive of each derivative and its spectrum profile.

Antimicrobial Activity Assays. *S. aureus* NCTC8325 and *E. coli* TOP 10 cells (5×10^5 cells·mL^{-1}) in Mueller−Hinton broth (MHB) media were exposed to each COM at the concentrations of 10, 100, and 1000 μg/mL (24 h, 37 °C, with continuous agitation). COMs were added to the media from a stock solution (50 mg/mL) in DMSO to a final concentration in media of 2% (v/v) of DMSO. The data on each COM antimicrobial effect integrate results obtained with three biological replicates having a distinct bacteria inoculum (each with three technical replicates), executed in nonconsecutive days. Negative controls (without COMs) were done with the same number of replicates. After 24 h, the antimicrobial effect was evaluated through colony-forming units (CFU) and medium turbidity (OD at 600 nm). Blanks for the OD measurements were conducted for each concentration/COM type (noninoculated).

Statistical Analyses. T-test paired analyses were performed using the analysis toolpak on excel ($p > 0.05$). A low variance within each source of cutin-rich materials (mg/g of each constituent monomer) was estimated through Levene's test: p-value = 0.9997, p-value = 0.9999 for material derived from POM^{I-II} and POM^{III-IV}, respectively. Accordingly, the dissimilarity between the two materials per monomer was analyzed using a one-way analysis of variance (ANOVA). The contributions of each chemical class and of each monomer to the overall difference between the materials were calculated using Principal Components Analyses (PCA) in R studio v.4.1.0. The statistical analyses were performed using the software XL-STAT v.2014.5.03 (Addinsoft).

RESULTS AND DISCUSSION

Tomato Pomace Chemical Variability: One or Many Raw Materials? The development of new value chains using residues from the agro-industry faces several technical challenges that are intrinsically related to their chemical complexity and heterogeneity. Geographically distant facilities usually rely on plant cultivars produced locally, generating residues with variable compositions: raw material and/or process-specific. To understand how such variation may impact the use of tomato pomace as a source material, the chemical composition of pomaces from tomato processing industries located in two different European countries was analyzed. Both pomaces were cryogenically milled to aid solubilization in DMSO-d_6 prior to NMR analysis. This strategy has been successfully applied to solubilize cork suberin directly from cork residues,[29] and to solubilize cutin from tomato peels.[22,28] The high-resolution ^{1}H NMR spectra of either pomace depict many overlapping signals (Figure S1), which are typically found in cutin isolated from peels.[22,28] The assignment of the NMR signals was attained through a combination of 2D spectra (^{1}H−^{1}H COSY, ^{1}H−^{13}C HSQC, and ^{1}H−^{13}C HMBC; Figures S2−S7), using as reference previous assignments in oligomeric/polymeric structures of cutin,[22,28,29,33] suberin,[28,29] and lignin.[34−36] The acquired HSQC spectra are shown in Figure 1, detailing the aliphatic and CH/CH$_2$-X aliphatics (A) and glycerol CH-acyl (B) regions, highlighting cutin signature signals (e.g., primary aliphatic esters, PAE). In the aliphatic region of both pomace spectra, methyl groups (CH_3) are present. The allylic groups (HC═CH−$\underline{CH_2}$) are assigned to δ_C/δ_H: 26.55/2.00 and 26.11/2.01; POM^{I-II} and POM^{III-IV}, respectively; characteristic of unsaturated fatty acids (UFA). Further signals related to UFA (H_2C═$\underline{CH}$═CH_2) are detected at δ_C/δ_H 25.16/2.72 and δ_C/δ_H 24.74/2.73 in POM^{I-II} and POM^{III-IV}, respectively. Tomato seeds contain significant amounts of UFA (e.g., octadeca-9,12-dienoic acid and octadec-9-enoic acid),[15,20,37] which may have contributed to the detected UFA signals in either pomace. Detailing key polymeric features, both spectra have a methylene group linked to the carbonyl of the ester bond (CH_2O(C═O)−$\underline{CH_2}$−), named α(C═O) esters (δ_C/δ_H: 33.36/2.27 and 32.99/2.27; POM^{I-II} and POM^{III-IV}, respectively). Signals of α(C═O) acids are also present (δ_C/δ_H: 33.57/2.17 and 33.27/2.19, POM^{I-II} and POM^{III-IV}, respectively). Finally, methylene groups associated with free hydroxyls ($\underline{CH_2}$−CH−(OH)−) are distinguishable at δ_C/δ_H 36.82/1.39.

The glycerol CH-acyl regions (Figure 1B) show the 1,2,3-triacylglycerol (TAG) configuration, differentiating in the POM^{I-II} and POM^{III-IV}, respectively, the signals of H_1 (δ_C/δ_H: 61.77/4.25; 61.28/4.25), H_3 (δ_C/δ_H: 61.71/4.11; 61.29/4.13), and H_2 (δ_C/δ_H: 68.72/5.18; 68.34/5.17). The TAG signal accounts for the contribution of triglycerides, which are abundant in the seed oil,[38] despite that it may also derive from solubilization of suberin extant in seed coating, of which glycerol is a monomeric constituent.[16,29] Ethyl-ester types are present in either spectrum (δ_C/δ_H: 65.67/4.03 and 65.40/4.05 in POM^{I-II} and POM^{III-IV}, respectively), similar to that reported before in tomato-processed samples (e.g., juices, purées, and pastes).[39,40]

Primary esters of the linear structures with a methylene group linked to the oxygen atom of the ester bond (−$\underline{CH_2}$−O−(C═O)),[22,29,33] named PAE-α, are apparent (δ_C/δ_H: 64.51/3.97 and 64.29/4.00, POM^{I-II} and POM^{III-IV}, respectively). The presence of PAE-α and the abundance in aliphatic constitute representative structures of cutin. In either pomace spectrum, free midchain hydroxyl groups ($\underline{CH_2}$−CH−(OH)−) are noted, comparable to that described before in tomato cuticle and the resultant cutin.[22] The NMR spectral fingerprints of the two pomaces are qualitatively highly comparable, both spectra being dominated by features associated with cutin. The pomace comprises mostly peels but also seeds and stems. Understanding in what manner the minor pomace's constituents influence the pomace chemical fingerprint secures knowledge-based advances in the formulation of cutin-derived products from underexploited tomato pomaces.

Tomato Pomace Chemical Fingerprint: Contemplating the Minor Constituents. To better understand the origin of the pomace chemical signature, the crude sample was fractionated into peels, seeds, and stems, selecting the POM^{III-IV} as a model. The resulting ^{1}H NMR spectra of the cryogenic milled fractions are depicted in Figure 1 (see detailed HSQC of the aromatic region for each fraction in Figure S8). The spectral aliphatic regions show that seeds and peels are more diverse in monomers containing methyl (CH_3) groups compared to stems. Stems are rich in acetyl groups (−OCO$\underline{CH_3}$) that can be found in carbohydrates associated with lignin.[34] All spectra contained allylic groups (HC═CH−$\underline{CH_2}$), but only those of peels and seeds contained signals characteristic of octadeca-9,12-dienoic acid (H_2C═$\underline{CH}$═

https://doi.org/10.1021/acssuschemeng.2c03437
ACS Sustainable Chem. Eng. 2022, 10, 11415−11427

Cutin-rich material extracted from:	POM^{I-II}	POM^{III-IV}
Alka(e)noic acids	**92.87 ± 8.99**	**115.55 ± 6.96**
Hexadecanoic acid	18.89 ± 1.42	47.19 ± 3.74
9,12-octadecadienoic acid	35.21 ± 4.41	12.25 ± 0.25
9-octadecenoic acid	24.68 ± 2.19	32.24 ± 1.38
Octadecanoic acid	14.1 ± 1.08	23.87 ± 1.77
ω-Hydroxyalka(e)noic acids	**603.82 ± 44.9**	**543.06 ± 27.18**
16-hydroxyhexadecanoic acid	18.7 ± 1.65*	21.32 ± 3.96*
10,16-Dihydroxyhexadecanoic acid	555.21 ± 40.1	483.61 ± 28.27
9,10-epoxy-18-hydroxyoctadecanoic acid	29.91 ± 3.91	38.13 ± 2.38
α, ω-Alkanedioic acids	**9.85 ± 1.29**	**56.4 ± 4.66**
Nonanedioic acid	n.d.	49.59 ± 3.74
Hexadecanedioic acid	9.85 ± 1.29*	10.21 ± 1.71*
Aromatics	**57.67 ± 14.1**	**29.87 ± 1.06**
4-hydroxybenzaldehyde	2.82 ± 0.16	3.02 ± 0.13
p-coumaric acid	24.66 ± 7.4*	26.85 ± 1.08*
Naringenin	30.19 ± 21.61	n.d.
Identification yield (%) - area	72.75 ± 0.97	66.42 ± 0.87

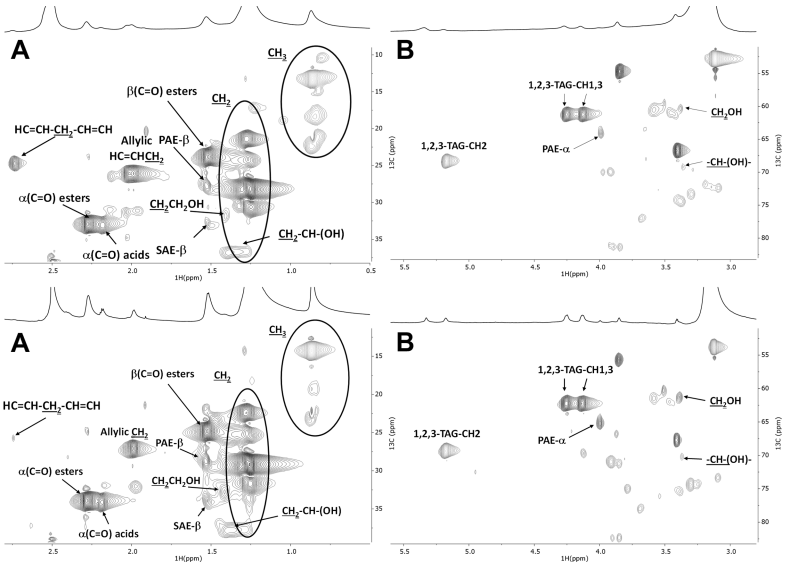

Figure 2. Compositional and spectral analysis of cutin-rich materials obtained from either pomace using an ionic liquid extractant. Quantitative analysis of the monomeric hydrolysates in either material by GC−MS (right table insert). The identification yields represent the ratio between the identified peak area and the total peak area in the chromatogram. Monomers having no statistical difference between the samples are marked with an asterisk (one-way ANOVA, $p > 0.05$). HSQC spectral characterization of each cutin-rich material, derived from POM^{I-II} (top panel) and POM^{III-IV} (bottom panel), detailing the aliphatic (A) and glycerol CH-acyl (B) regions. Some assignments (unlabeled) are uncertain or unidentified. Results are given as mg of compound per g of starting material.

CH_2), which besides being a cutin monomer is highly abundant in seeds.

The peels contained assignments related to PAE-β and SAE-β (glycerol CH-acyl region). These signals together with the chemical signature of the aliphatic region confirmed, as expected, that peels are the source of cutin extant in the pomace. Also, secondary free hydroxyl groups (−CH−(OH)−) were assigned in peels found in tomato cutin.[18,22] On the contrary, the TAG signal could be only assigned in seeds, confirming that its detection in either pomace originates from this fraction. The seeds display as well signals of methyl- and ethyl-ester signals, $\underline{CH_3}$-ester and $CH_3-\underline{CH_2}$-ester, respectively. Both seeds and peels present signals assigned to alkene groups (aromatic region), consistent with their composition, having waxes and fatty acids that are rich in these groups.[4,37,41]

Stem's spectrum shows signals related to β-aryl ether units (Cα/Hα; Cβ/Hβ; Cγ/Hγ), β-D-xylopyranoside units (C_3-H_3; C_2-H_2), and methoxyls ($-OCH_3$) that are typical of the lignin polymer.[34,36,42] Signals related with β-D-xylopyranoside units (C_3-H_3;2,3.-O-acetyl-β-D-xylopyranoside;2-O-acetyl-β-D-xylopyranoside), syringyl units ($C_{2,6}-H_{2,6}$; S′, syringyl), guaiacyl units (C_2-H_2) and other glycoside linkages (xylan 2-O-Ac-β-D-Xylp; xylan;(1 → 4)-β-D-Manp; 4-O-methyl-α-D-GlcUA) could be assigned in the aromatic region. All assignments have been associated before with lignin.[34−36]

The acquired data indicate that seeds and stems are adding complexity to the pomace NMR spectra since those fractions present higher contributions in the glycerol CH-Acyl and aromatics regions. Peels otherwise are mainly composed of aliphatic moieties (CH_2 and CH_3 groups), with alcohol, acids, and ester bonds associated. Besides, only peels show the SAE-β signal in the glycerol CH-acyl region (Figure 1B), a distinctive feature of the chemical fingerprint of tomato peel.

Cutin Isolation from Pomaces: Cutin Structure Is Highly Source-Specific. Cutin can be isolated from tomato cuticles using as extractant the ionic liquid cholinium hexanoate.[22] It allows a swift and uncomplicated recovery of a cutin polymer with minor structural alterations. Inspired by these results, cutin-rich materials were obtained from each pomace using the same process.[22] The HSQC spectra of the isolated materials display apparently reduced heterogeneity compared to the starting pomaces (Figures 2 and S9). The presence of aliphatics (CH_2 and CH_3), α and β(C═O) esters, primary and secondary free hydroxyl groups ($CH_2\underline{CH_2}OH$ and $CH_2-\underline{CH}-(OH)$), PAE, and SAE (both α- and β-configurations) in either spectrum matches the chemical fingerprint observed herein in the peels' spectrum (Figure 1, bottom panel), and that reported before for cutin isolated from peels using the same process.[22,33] The exception is the presence of the TAG configuration in either cutin-rich material. This observation suggests that suberin structures derived from seeds were co-extracted with cutin because most seed triglycerides are most likely washed out during cutin recovery. The abundances of each hydrolyzable monomer in either ionic liquid extracted material were quantified by GC−MS (table insert in Figure 2). In general, both materials show the typical composition of hydrolyzable monomers for tomato cutin,[21,22,33] with ω-hydroxyalkanoic acids as the most abundant class, in particular 10,16-dihydroxyhexadecanoic acid. The diversity/abundance of the remaining hydrolyzable monomers shows a specific signature dependent on the source of the material, most of them (mg/g of material) contributing to the materials' clear statistical separation (PCA, Figure S9A). This observation is consistent with previous data showing that the monomeric composition of cutin from tomato peel is greatly influenced by the cultivar, cultivation conditions, and fruit ripening state, among other factors.[43−45] The more relevant differences are the high abundance of naringenin in the cutin from the POM^{I-II} ($p = 0.0065$) and of nonanedioic acid in the hydrolyzed cutin from the POM^{III-IV} (undetectable in the counterparts, $p < 0.0001$). Finally, the amount of

https://doi.org/10.1021/acssuschemeng.2c03437
ACS Sustainable Chem. Eng. 2022, 10, 11415−11427

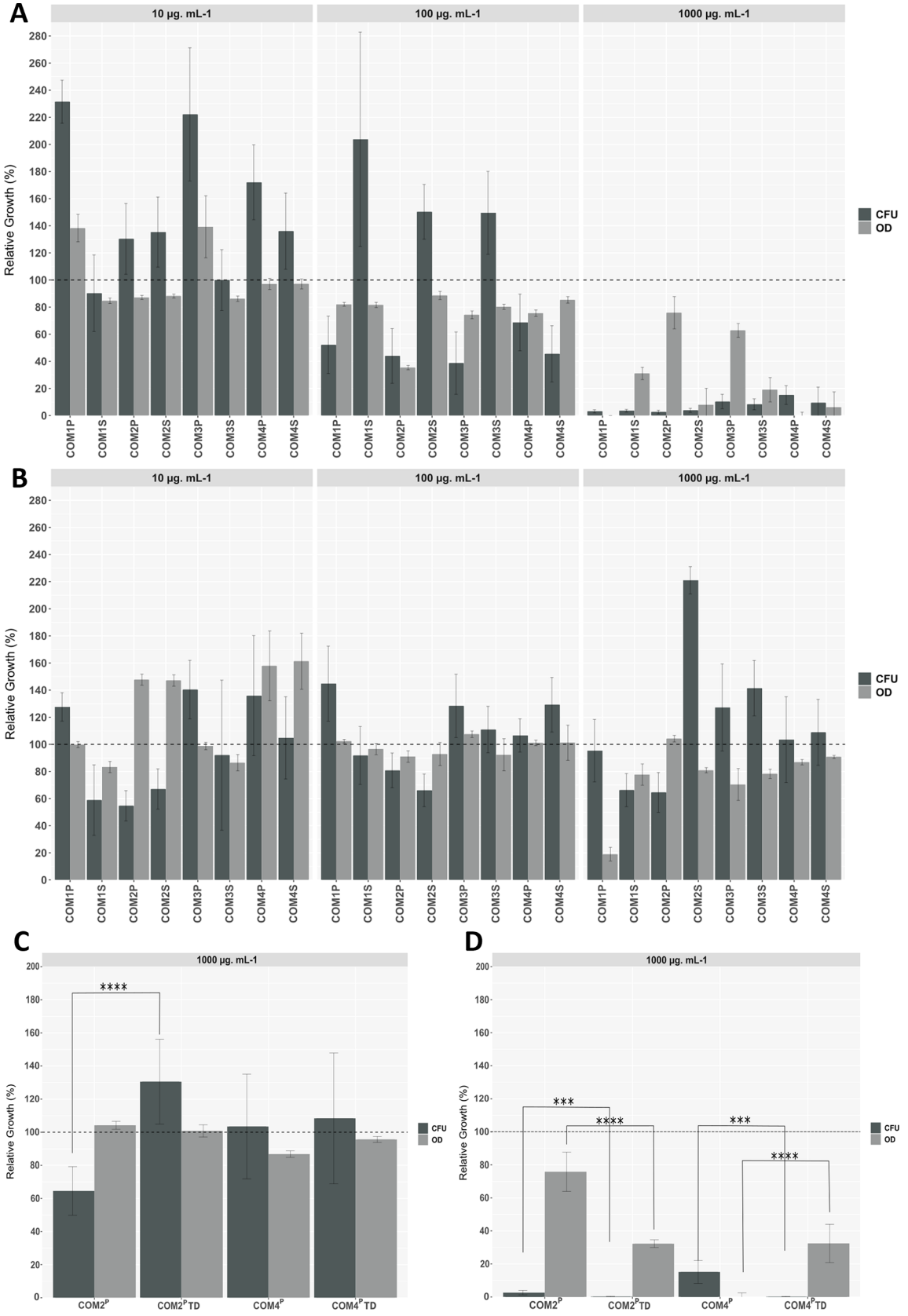

Figure 3. Screening of all COMs bactericidal activity against *S. aureus* (A, C) and *E. coli* (B, D). Bacterial growth evaluated through measurements of media turbidity (OD_{600}, gray bars) and colony-forming units (CFU, dark bars), both presented as the % relative to the corresponding negative control. The dashed line at 100% represents the control for both assays. The error bar represents the standard deviation between replicates. The bactericidal activity of $COM2^P$ and $COM4^P$ after total depolymerization (TD) against *S. aureus* (C) and *E. coli* (D) was analyzed as well. Significant changes are marked (*t*-test, $p < 0.05$; *$p \leq 0.05$; **$p \leq 0.01$; ***$p \leq 0.001$; ****$p \leq 0.0001$).

https://doi.org/10.1021/acssuschemeng.2c03437
ACS Sustainable Chem. Eng. 2022, 10, 11415−11427

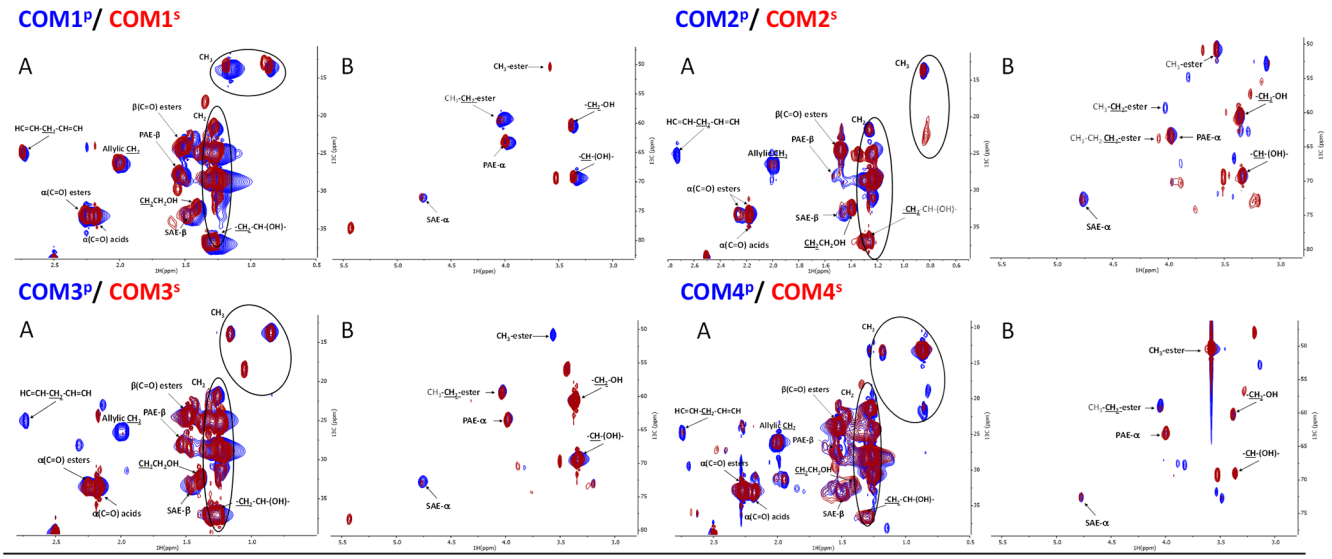

	PAE (%) [i]	SAE (%) [i]	Methyl-PAE (%) [i]	Ethyl-PAE (%) [i]	Total Esters [ii]	^{31}P NMR quantification (mmol/g)
COM1^{P}	**21.32** ± 0.92 **[0.83]**	**18.30** ± 7.13 **[0.71]**	**0.85** ± 0.75 **[0.03]**	**59.53** ± 6.34 **[2.32]**	**3.90** ± 0.27	Free acids **0.59** ± 0.03 OH aliphatics **2.58** ± 0.12 OH aromatics **0.92** ± 0.04
COM1^{S}	**60.61** ± 5.32 **[1.35]**	**14.46** ± 18.02 **[0.32]**	**24.93** ± 22.00 **[0.55]**	n.d. **[0.00]**	**2.22** ± 0.64	Free acids **2.34** ± 0.37 OH aliphatics **3.99** ± 0.64 OH aromatics **0.79** ± 0.12
COM2^{P}	**9.65** ± 0.22 **[0.30]**	**18.38** ± 3.29 **[0.58]**	**28.86** ± 3.27 **[0.91]**	**43.12** ± 2.38 **[1.36]**	**3.16** ± 0.83	Free acids **0.59** ± 0.05 OH aliphatics **0.57** ± 0.07 OH aromatics **0.05** ± 0.01
COM2^{S} [iii]	**18.60** ± 8.58 **[0.32]**	**19.49** ± 13.06 **[0.33]**	**55.01** ± 28.71 **[0.94]**	n.d. **[0.00]**	**1.70** ± 1.23	Free acids **1.30** ± 0.30 OH aliphatics **1.56** ± 0.17 OH aromatics **0.15** ± 0.04
COM3^{P}	**28.14** ± 5.42 **[0.78]**	**34.76** ± 2.71 **[0.96]**	**17.46** ± 2.27 **[0.48]**	**19.64** ± 6.00 **[0.54]**	**2.77** ± 0.17	Free acids **1.46** ± 0.27 OH aliphatics **1.49** ± 0.28 OH aromatics **0.48** ± 0.10
COM3^{S}	**35.98** ± 4.77 **[1.20]**	**16.81** ± 2.11 **[0.56]**	**1.93** ± 1.67 **[0.06]**	**45.28** ± 5.12 **[1.50]**	**3.32** ± 1.37	Free acids **1.99** ± 0.12 OH aliphatics **3.88** ± 0.30 OH aromatics **0.56** ± 0.05
COM4^{P}	**14.13** ± 5.76 **[0.54]**	**23.30** ± 7.58 **[0.88]**	**39.82** ± 22.16 **[1.51]**	**22.75** ± 8.84 **[0.86]**	**3.79** ± 0.80	Free acids **1.66** ± 0.30 OH aliphatics **1.00** ± 0.14 OH aromatics **0.08** ± 0.04
COM4^{S}	**28.43** ± 15.64 **[0.88]**	**13.24** ± 8.22 **[0.41]**	**58.33** ± 20.36 **[1.81]**	n.d. **[0.00]**	**3.11** ± 0.14	Free acids **3.25** ± 0.10 OH aliphatics **1.72** ± 0.07 OH aromatics **0.06** ± 0.02

Figure 4. Spectral characterization of each COM (HSQC spectra, detailing the aliphatic (A) and glycerol CH-acyl (B) regions; top panel) and quantification of primary and secondary aliphatic esters (and primary ester types) and the amount of free acids, OH aliphatics and OH aromatics as well (estimated using ^{31}P NMR) (bottom table). Some assignments (unlabeled) are uncertain or unidentified.

hydrolyzable carbohydrates (acidic hydrolysis, Table S1) in either cutin-rich material is at the ppm level. This observation, together with the monomeric fingerprint of either material shows the superior capacity of the ionic liquid to extract from the untreated pomace almost exclusively cutin, with a minor contribution of suberin and other lipids from seeds. Based on the data, it is hypothesized that the pattern of oligomers obtained through mild hydrolyses of each cutin-rich material may still retain source-specific features.

Cutin-Rich Materials from Pomaces: Breaking the Cutin Wall to Release Antimicrobial Bricks. Monomeric fatty acid constituents of cutin including hydroxy and dicarboxylic derivatives, as well as its aromatic monomers, can show bactericidal activity.[46−50] Activity of fatty acids is structure-dependent; medium-/long-chain fatty acids, especially unsaturated ones, are active against Gram+ (usually not against Gram− that are more susceptible to short-chain fatty acids).[46−48] Their methyl ester derivatives show usually decreased activity.[48] Dicarboxylic fatty acids show lower bactericidal activity, possibly due to the presence of polar groups at both ends of the fatty acid chain, regardless that unsaturated C_{16} and C_{18} dioic acids are reported to possess great antimicrobial activity.[51] In addition, suberin particles consisting of esterified polymeric structures own bactericidal properties.[29] It can be hypothesized that bactericidal esterified cutin structures can also be obtained from cutin-rich materials extracted from tomato pomace. Mild hydrolysis of cutin can release oligomers composed of ≥7 monomers.[33,52] As such, either material was hydrolyzed herein by two different methods to generate cutin oligomeric mixtures (COMs 1 and 2 from the

https://doi.org/10.1021/acssuschemeng.2c03437
ACS Sustainable Chem. Eng. 2022, 10, 11415−11427

Table 1. Quantitative Analysis of Hydrolyzable Monomers Comprising Each COM by GC−MS[a]

	COM1^{P}	COM1^{S}	COM2^{P}	COM2^{S}
alka(e)noic acids	48.17 ± 7.49	26.1 ± 3.31	339.63 ± 40.61	203.23 ± 11.79
hexadecanoic acid	8.4 ± 0.85	6.94 ± 0.81	52.94 ± 2.6	37.73 ± 1.8
9,12-octadecadienoic acid	21.18 ± 5.99	6.89 ± 1.37	170.7 ± 39.13	86.01 ± 4.96
9-octadecenoic acid	12.8 ± 1.02	5.4 ± 0.7	84.87 ± 7.7	53.09 ± 3.6
octadecanoic acid	5.79 ± 0.57	6.86 ± 0.84	31.12 ± 3.24	26.4 ± 2.04
ω-hydroxyalkanoic acids	288.36 ± 21.94	257.14 ± 34.99	110.21 ± 15.63	182.86 ± 10.33
16-hydroxyhexadecanoic acid	10.6 ± 1.13	5.32 ± 0.6	14.35 ± 0.56	18.16 ± 1.39
10,16-dihydroxyhexadecanoic acid	263.24 ± 20.64	234.11 ± 32.61	82.03 ± 14.78	156.75 ± 7.66
9,10-epoxy-18-hydroxyoctadecanoic acid	14.52 ± 1.35	17.7 ± 2.49	13.83 ± 0.48	23.86 ± 0.52
α,ω-alkanedioic acids	5.54 ± 2.11	18.35 ± 4.48	8.27 ± 4.31	51.85 ± 1.97
octanedioic acid	n.d.	1.58 ± 0.36	n.d.	n.d.
nonanedioic acid	1.06 ± 0.04	16.77 ± 4.12	3.68 ± 0.13	39.49 ± 0.9
hexadecanedioic acid	4.83 ± 2.07	n.d.	6.98 ± 0.61	12.36 ± 1.33
aromatics	1.65 ± 0.5	2.86 ± 1.04	5.33 ± 0.46	13 ± 0.59
4-hydroxybenzaldehyde	0.19 ± 0.07	0.23 ± 0.06	n.d.	3.77 ± 0.44
p-coumaric acid	1.03 ± 0.13	1.87 ± 0.92	5.33 ± 0.46	9.23 ± 0.19
naringenin	0.52 ± 0.41	0.76 ± 0.12	n.d.	n.d.
identification yield (%)—area	84.04 ± 2.90	80.98 ± 4.53	87.16 ± 9.33	67.90 ± 2.22
	COM3^{P}	COM3^{S}	COM4^{P}	COM4^{S}
alka(e)noic acids	144.15 ± 12.77	10.29 ± 3.08	330.82 ± 43.12	70.04 ± 3.51
hexadecanoic acid	35.84 ± 0.96	3.47 ± 0.64	145.17 ± 21.54	20.5 ± 2.47
9,12-octadecadienoic acid	42.09 ± 1.09	2.52 ± 0.24	33.72 ± 3.31	15.33 ± 0.8
9-octadecenoic acid	49.33 ± 13.22	2.67 ± 0.23	106.22 ± 13.75	24.15 ± 1.74
octadecanoic acid	16.88 ± 0.38	2.92 ± 0.49	45.7 ± 5.17	12.07 ± 0.6
ω-hydroxyalkanoic acids	309.65 ± 4.19	552.52 ± 61.77	187.18 ± 22.6	136.08 ± 19
16-hydroxyhexadecanoic acid	21.82 ± 0.48	3.25 ± 0.34	16.94 ± 1.1	n.d.
10,16-dihydroxyhexadecanoic acid	265.2 ± 4.39	512.91 ± 53.19	150.32 ± 19.98	136.08 ± 19
9,10-epoxy-18-hydroxyoctadecanoic acid	22.63 ± 1.23	37.44 ± 7.37	19.91 ± 1.71	n.d.
α,ω-alkanedioic acids	16.11 ± 1.2	153.6 ± 44.21	27.81 ± 5.41	219.38 ± 28.92
octanedioic acid	n.d.	8.36 ± 3.1	n.d.	22.73 ± 2.85
nonanedioic acid	4.86 ± 0.5	145.24 ± 41.13	16.52 ± 3.91	189.93 ± 24.96
hexadecanedioic acid	11.26 ± 0.72	n.d.	11.29 ± 1.54	6.72 ± 1.43
aromatics	21 ± 1.93	20.13 ± 4.32	6.55 ± 0.97	8.04 ± 1.52
4-hydroxybenzaldehyde	4.15 ± 0.14	2.64 ± 0.5	n.d.	3.19 ± 0.04
p-coumaric acid	14.81 ± 1.34	13.38 ± 2.55	6.55 ± 0.97	6.45 ± 0.53
naringenin	6.12 ± 0.54	4.12 ± 1.51	n.d.	n.d.
identification yield (%)—area	72.57 ± 6.72	83.91 ± 1.22	71.98 ± 0.81	46.85 ± 5.27

[a]Results are given as mg of compound per g of starting material. The identification yields are indicated below and represent the ratio between the identified peak area and the total peak area in the chromatogram. Monomers that were not detected in a specific sample are labeled as n.d.

POM^{I-II}; 3 and 4 from the POM^{III-IV}), each subsequently split into precipitated—COM^{P}—and soluble—COM^{S}—fractions (see the Materials and Methods section).

To test the working hypothesis that within cutin-rich materials are walled diverse bactericidal esterified structures (apart from active monomers against Gram+ bacteria), the COMs' capacity to impact bacterial viability was tested (10, 100, and 1000 $\mu g \cdot mL^{-1}$). Specifically, two model bacterial strains were used: *E. coli*—a Gram− bacterium and *S. aureus*—a Gram+ bacterium. Cellular viability was directly measured by the numbers of colony-forming units compared to control (without COMs), whereas the medium turbidity (OD_{600}), also relative to the control, taken together with the viability measurements provides clues on bacterial integrity upon exposure. Collectively, the results showed striking different source- and concentration-dependent bactericidal effects against the two bacteria (Figure 3). Some data points present high variability between replicates, presumably due to the COMs' heterogeneity.

COMs bactericidal activity against *S. aureus* increased proportionally with concentration (regardless of the pomace source), reducing bacterial growth by 84 and 97% at the highest tested concentration (Figure 3A). Reduction of the media turbidity, followed, in general, the same trend of cellular viability, and hence suggesting that dead cells suffered lysis, except for COM1^{S}, COM2^{P}, and COM3^{P}, where media turbidity values were still high. The impact of COMs in the media turbidity (e.g., due to spontaneous lipid-based vesicle formation) was discounted.

Contrarily to that observed in *S. aureus*, COMs' activity against *E. coli* was source-dependent. In brief, none of the COMs derived from the POM^{III-IV} (COM 3 and 4) were able to impact *E. coli* growth at all tested concentrations. On the contrary, the COMs derived from the POM^{I-II} (COM 1 and 2) could reduce, to some extent, *E. coli* viability, except COM1^{P} (Figure 3B). However, their activity did not show a linear dependence of the concentration, achieving, in general, the highest viability reduction at the lowest concentration (≥45%). For the two COM2 samples, the media turbidity

https://doi.org/10.1021/acssuschemeng.2c03437
ACS Sustainable Chem. Eng. 2022, 10, 11415−11427

showed an opposing trend of viability reduction. This observation suggests that they altered *E. coli* cellular morphology, e.g., growth of an elongated phenotype. This stress response phenomenon was observed for *E. coli* cells exposed to suberin particles at sub-inhibitory concentrations, and hence may deserve focused analysis in the future.[29]

Each COM was quantitatively analyzed by NMR, specifically ^{31}P NMR was used to quantify the extant amounts of free acid and hydroxyl groups,[53] and ^{1}H NMR with an internal standard was used to quantify the amounts of each ester type (Figures 4 and S11−S30). The HSQC spectra illustrate that all COMs contain cutin oligomers linked through PAE and SAE esters. Methyl esters are formed during the two hydrolyses due to the use of methanol (more efficiently in the methanolysis, though), and were visible in all spectra, except for COM1^{P} and COM3^{S} (likely below the detection threshold) (Figure 4). The presence of ethyl esters in all samples, except COM2^{S}, is an artifact since ethanol was used in sample preparation. Finally, propyl esters were detected only in the spectrum of COM2^{S} (absent in the GC−MS analysis, see below); its origin cannot be explained by the used methods.

The presence of TAG in the spectra of either cutin-rich material (Figure 4) highlights that some suberin was co-extracted with cutin from the pomaces (Figure 2), despite that contamination with seed triglycerides cannot be disregarded. To verify if suberin contributes to the chemical diversity of the COMs, seeds and peels (from POM^{III-IV}) were processed with the ionic liquid to recover polyester-rich materials. Those materials were hydrolyzed (sodium hydroxide mediated hydrolysis). The HSQC spectra of the ensuing oligomeric mixtures (Figure S31) show some overlapping features (e.g., PAE; $\underline{CH}$−(OH)−; −$\underline{CH_2}$−OH) but SAEs are only visible in those derived from peels. This signal therefore constitutes the most differentiating factor as it is specifically linked to peels, and hence to cutin as well (Figure 1). Besides, the TAG signal, specific of seeds, is absent (Figure 2). These results suggest that all COMs' oligomers obtained from the cutin-rich materials derived mostly from cutin. The contribution of the quantifiable NMR features to the dissimilarity of the different COMs was statistically evaluated using Principal Components Analysis (Figure S32). The results showed that their dissimilarity is mostly associated with the abundance of SAE and PAE and the amount of methyl esters as well, and hence with separation of samples *per* hydrolysis type (PC1) and *per* fraction, namely, soluble and precipitate (PC2).

COM2^{P} (active against either bacterium) was selected to investigate if the presence of ethyl esters (an artifact introduced by the reagent ethanol) influences activity. A new sample—COM2^{P}Ø—was prepared using dichloromethane instead of ethanol, having similar chemical composition to COM2^{P}. The results show that the presence of ethyl esters did not significantly affect bioactivity against either bacterium (pairwise *t*-test $p > 0.05$ for all) (Figure S33).

The results show that bactericidal "cutin-bricks" can be isolated from either source, effective and concentration-dependent against *S. aureus*, but also active against *E. coli*, highly source-dependent and showing modest but promising bacteria viability reductions. The data suggest that esterification is essential for activity against the Gram− bacterium (e.g., COM2^{P}) but is not the only required feature as some COMs containing esterified structures were inactive (e.g., COM3^{P}). Further chemical analyses are required to identify the key players for the observed activity, hindered by the complexity of the COMs, comprising not a single chemical entity but a complex mixture.

Cutin Oligomeric Mixtures: Searching for Source-Specific Features That May Increase Antimicrobial Properties, A Needle in a Haystack. The diversity/abundance of free monomers extant in either COM can impact the bactericidal effect of the mixtures.[48,54−57] All COMs were observed to contain free monomers (GC−MS analyses, Tables S2 and S3) comprising ca. 25−40% of the total COMs' mass, except COM3^{S} of which free monomers were 58 wt %. In all cases, alka(e)noic acids are consistently the more abundant free monomers present in the COMs, except in COM1^{S} and COM3^{S} where ω-hydroxyalkanoic acids are more abundant instead. Total depolymerization of either COM (through alkaline hydrolysis) was used to break down the oligomers (i.e., to release their composing hydrolyzable monomers, Table 1). This may lead to the loss of some free monomers in the aqueous phase. Nonetheless, after the breakdown of the extant oligomers, the mass of identified monomers generally increased (Tables S2 and S3), consistent with the NMR data that show the presence of PAE and SAE. As a result of such inherent technical limitations, the precise fingerprint of the extant oligomeric structures remains unknown. Though the PCA analysis of the NMR data was able to separate COMs *per* hydrolysis/fraction type (Figure S31), their monomeric compositional fingerprints (attained with the COM's hydrolysates) did not show any obvious pattern of association, except that replicates were clustered together (Figure S33).

The maximum concentrations of each free monomer in the COM were compared with the published minimal inhibitory concentrations (MICs, mM) against *S. aureus* and *E. coli* (Table S4).[46−48,56] The data show that the free amounts of 9−12-octadecadienoic acid (linoleic acid) in COM2^{P} and COM2^{S}; and of 9-octadecenoic acid (oleic acid) in COM4^{P} could explain the observed bioactivity against *S. aureus*. For the remaining COMs, their concentrations, and of other known bioactive monomers as well (e.g., *p*-coumaric acid, nonanedioic acid), are all below the MICs reported in other studies, irrespectively that synergies between different compounds might influence the activity of the mixture. Accordingly, after depolymerization, COM2^{P} and COM4^{P} (1000 $\mu g \cdot mL^{-1}$) showed a small yet statistically relevant increase (inferred by the reduction of CFUs) of bactericidal potency against *S. aureus* (Figure 3C). For both samples, the medium-turbidity data suggest that breaking down the oligomeric structures might have altered the bactericidal mode of action against *S. aureus*. On the contrary, depolymerization of COM2^{P} decreased greatly its efficacy against *E. coli*, whereas COM4^{P} remained inactive (Figure 3D).

Analysis of the ratio of each monomer amount before depolymerization (i.e., free monomers present in the COM) to its amount after depolymerization (i.e., all free monomers, including those linked prior to depolymerization) (Figure S35) was used to indicate candidate building blocks of oligomeric structures. An additional feature that might influence activity is the amount of PAE (i.e., linear) and SAE (i.e., branched) (insert table in Figure 4). Importantly, different compounds may contribute to the activity of different COMs. Taken as an example of the bioactive oligomers against *E. coli*, both COM2^{P} and COM1^{S} likely comprise key building block 10−16-dihydroxydecanoic acid (ratio >10 and 1 < ratio < 3, respectively). COM2^{P} has 2-fold more SAE than PAE, whereas

https://doi.org/10.1021/acssuschemeng.2c03437
ACS Sustainable Chem. Eng. 2022, 10, 11415−11427

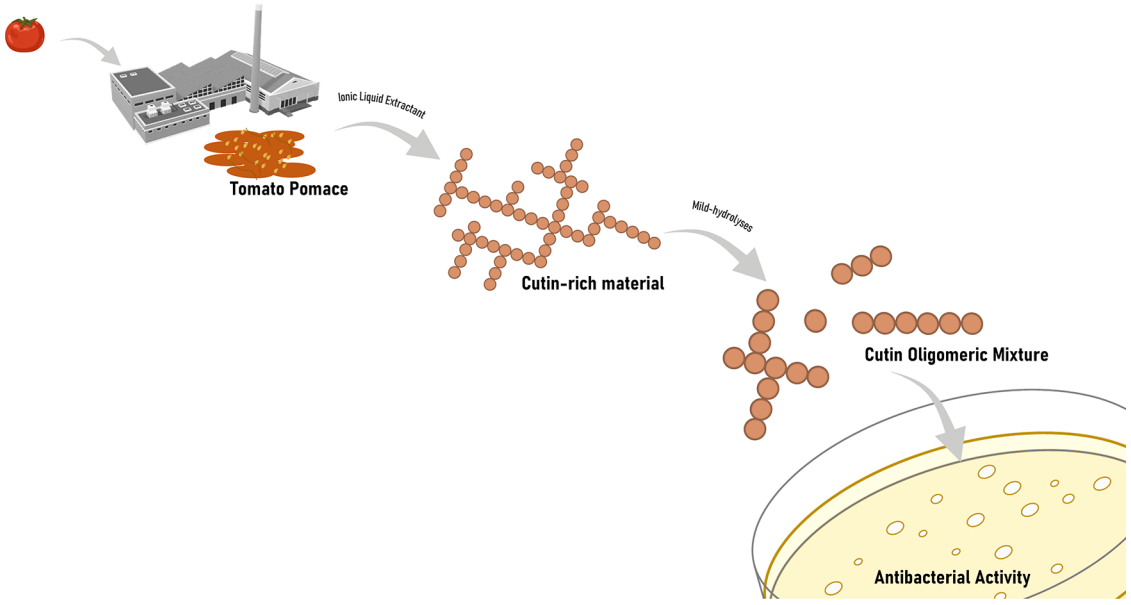

Figure 5. Schematic for the production of bactericidal cutin oligomeric mixtures through mild hydrolyses of cutin-rich materials obtained directly from crude tomato pomace using an ionic liquid extractant.

COM1^{S} has 4-fold more PAE than SAE. COM2^{S} active oligomers have nonanedioic acid as a candidate building block (3.1 < ratio < 7) having similar amounts of both ester types.

To correlate the COM's chemistry with the observed activities against *S. aureus* is somehow nonsense as all samples were active, showing a concentration-dependent effect. Besides, COMs were active even after depolymerization, suggesting a major role of free monomers for the observed activity. One particularity of all COMs derived from the POM^{III-IV} is that they comprise oligomers likely containing aromatic compounds, possibly with some ownership of activity against *S. aureus*, more obvious for COM3. This observation also questions if aromatics are covalently bound to cutin as suggested before.[58]

Any pomace constitutes suitable sources for cutin-rich material to be subsequently deconstructed to produce bactericidal bricks against *S. aureus*. However, for the production of mixtures active against *E. coli*, cutin-rich materials having low levels of hydrolyzable dioic acids gave the most promising results. Both mild depolymerization methods have rendered active mixtures against both bacteria, but the precipitated fractions contain lower amounts of free monomers deserving focused analysis soon.

CONCLUSIONS

The availability of fruit pomace generated as waste side-streams by numerous and diverse agro-food industries raises outstanding questions: What hidden values hold these complex heterogeneous waste streams? Are there major compositional traits that allow us to better discriminate processing routes that align with circular bio-economy? This study starts answering these questions, contributing to altering the status quo of tomato pomace. It is readily available at tons' levels, mostly seasonally, having high heterogeneity due to major differences both in the processing methods and the processed source, i.e., tomato fruit.[15] The first working hypothesis is obvious: all-inclusive decoding of the pomace's chemistry can distinguish correlations between its major compositional traits with those of the derived cutin-rich materials, and the afterward produced cutin oligomeric mixtures—COMs. Spectroscopic analyses show that tomato pomaces obtained at distinct industries display qualitatively high spectral similarity, with many signature signals associated with cutin—the major composing polymer of the fruit's cuticle—but also other unrelated signals (Figure 1, top). Deconvolution of the contribution of each pomace constituent—peels, seeds, and stems—to the pomace spectra, revealed that part of the chemical heterogeneity is due to the presence of seeds and stems (Figure 1, bottom). The latter adds to the pomace spectra, features which are usually assigned to polysaccharides and lignin. The contribution of seeds mostly expands the diversity of signals assigned to fatty acids, including acylglycerol fatty acids. Peels and seeds have as distinctive spectral features the presence of PAE in both and of SAE exclusively in peels. The acquired NMR data redefined the working hypothesis: the chemical specificities of each pomace will be partially lost during the preparation of cutin-rich materials. To obtain the materials, ionic liquid extraction was applied; one-pot reaction recovers an insoluble cutin continuum while washing out most of the noncutin materials. The ionic liquid extractant had outstanding performance: >55 wt % recovery yield (Table S5), retrieving a material displaying all archetypal spectral features of cutin pure materials, regardless of a minor contribution of constituents from seeds (as denoted by the TAG signal, Figure 2). Each cutin-rich material showed a unique fingerprint of hydrolyzable monomers (Figure 2). A third hypothesis was elaborated: mild depolymerization of cutin-rich materials having distinct compositional fingerprints will release diverse oligomers/monomers displaying broad bactericidal activity. The acquired data show that either source material can be used to generate COMs active against *S. aureus* (model Gram+ bacterium), all of which showed a concentration-dependent effect (Figure 3A). However, not all mixtures were able to kill *E. coli* (model Gram− bacterium) (Figure 3B); activity is correlated with the presence of oligomers (containing both PAE and SAE) possibly consisting of dioic acids (though not exclusively) (Figure S35). It was the material having more hydrolysis-resistant dioic acids (Figure 2) that rendered the mixtures

https://doi.org/10.1021/acssuschemeng.2c03437
ACS Sustainable Chem. Eng. 2022, 10, 11415−11427

more active against *E. coli* (Figure 3B). Importantly, for the large majority of the COMs tested herein, the observed activities against either model bacterium cannot be simply explained by the presence of free bioactive monomers (Table S4). Further studies are required to better correlate the chemistry of a cutin-rich material with that of the produced COMs, answering if optimal deconstruction of broad bactericidal structures walled in cutin can be defined for all cutin-rich pomace types.

Due to the high chemical complexity of the generated COMs, the contribution of each chemical entity to the observed activities remains obscure. However, it is clear that tomato pomace can produce bactericidal mixtures, exploring mild depolymerization of the derived cutin-rich materials. Future optimization of the depolymerization methods will seek to increase its greenness, e.g., using enzyme-mediated catalyzes.[59] Past studies showed that the ionic liquid extractant can be recovered upon water removal and reused,[60] but recent advances suggest that alternative methods can be applied instead, such as membrane (micro)filtration.[61,62] Finally, mass balance analysis of the process demonstrates that mild hydrolysis of the cutin-rich materials produced per hydrolytic round yields of 57 and 7.3 wt % of COMs for alkaline hydrolysis and methanolysis, respectively, whereas a new hydrolytic round of the nonhydrolyzed leftovers yields 15 and 26 wt % of COMs (Table S5). This observation shows that process optimization/intensification can further increase the production yields, regardless that further development and complementary techno-economic analyses are required.

In conclusion, this study constitutes proof of concept of a tomato pomace processing strategy for the production of bactericidal mixtures active against both Gram+ and Gram− bacteria (Figure 5). The presence of certain structural and compositional elements in the COMs is required for efficacy against the latter, e.g., PAE/SAE. Either pomace rendered high yields of a cutin-rich material through an uncomplicated ionic liquid extraction. The details supporting the sustainability of the proposed process are the absence of pretreatment of the pomace (it can be simply air-dried) and the chosen ionic liquid, which is biodegradable, biocompatible, and can be recycled and reused. Using stringent safe and sustainable design criteria, further optimization will be sought out seeking to contribute to the circular economy through the creation of new value chains for the tomato industry.

■ ASSOCIATED CONTENT

Supporting Information

The Supporting Information is available free of charge at https://pubs.acs.org/doi/10.1021/acssuschemeng.2c03437.

NMR spectra; GC−MS data; quantification tables and figures; and antimicrobial data (PDF)

■ AUTHOR INFORMATION

Corresponding Author

Cristina Silva Pereira − *Instituto de Tecnologia Química e Biológica António Xavier, Universidade Nova de Lisboa (ITQB NOVA), 2780-157 Oeiras, Portugal;* orcid.org/0000-0002-6750-1593; Email: spereira@itqb.unl.pt

Authors

Rita Escórcio − *Instituto de Tecnologia Química e Biológica António Xavier, Universidade Nova de Lisboa (ITQB NOVA), 2780-157 Oeiras, Portugal;* orcid.org/0000-0003-3473-3686

Artur Bento − *Instituto de Tecnologia Química e Biológica António Xavier, Universidade Nova de Lisboa (ITQB NOVA), 2780-157 Oeiras, Portugal;* orcid.org/0000-0003-4097-1613

Ana S. Tomé − *Instituto de Tecnologia Química e Biológica António Xavier, Universidade Nova de Lisboa (ITQB NOVA), 2780-157 Oeiras, Portugal;* orcid.org/0000-0002-5152-7908

Vanessa G. Correia − *Instituto de Tecnologia Química e Biológica António Xavier, Universidade Nova de Lisboa (ITQB NOVA), 2780-157 Oeiras, Portugal;* orcid.org/0000-0002-7357-7199

Rúben Rodrigues − *Instituto de Tecnologia Química e Biológica António Xavier, Universidade Nova de Lisboa (ITQB NOVA), 2780-157 Oeiras, Portugal*

Carlos J. S. Moreira − *Instituto de Tecnologia Química e Biológica António Xavier, Universidade Nova de Lisboa (ITQB NOVA), 2780-157 Oeiras, Portugal;* orcid.org/0000-0002-7708-2505

Didier Marion − *Research Unit Biopolymers Interaction Assemblies, INRAE, 44316 Nantes, France*

Bénédicte Bakan − *Research Unit Biopolymers Interaction Assemblies, INRAE, 44316 Nantes, France*

Complete contact information is available at: https://pubs.acs.org/10.1021/acssuschemeng.2c03437

Author Contributions

C.S.P. contributed to conceptualization, funding acquisition, project administration, and supervision). C.S.P., B.B., and D.M. contributed to resources. R.E., A.B., and C.J.S.M. performed ionic liquid synthesis, cutin extraction, and cryogenic milling. R.E. and A.B. carried out cutin hydrolyses. R.E. and A.B. performed NMR data analyses. A.S.T. conducted GC−MS analyses. R.E., R.R., and V.G.C. performed antimicrobial activity tests. A.S.T., R.E., and V.G.C. carried out statistical analyses. R.E. prepared the initial draft of the manuscript. All authors read and approved the final version of the manuscript.

Notes

The authors declare no competing financial interest.

■ ACKNOWLEDGMENTS

The authors acknowledge funding from the European Research Council through grant ERC CoG-647928, from the European Union's Horizon 2020 research and innovation program within the project 713475−FLIPT−H2020-FETOPEN-2014−2015, and from Fundação para a Ciência e Tecnologia (FCT) by Project MOSTMICRO ITQB with refs UIDB/04612/2020 and UIDP/04612/2020. R.E. is grateful to FCT funding for her PhD scholarship (2021.06435.BD). The NMR data were acquired at CERMAX, ITQB-NOVA, Oeiras, Portugal, with equipment funded by FCT. The authors are thankful to Daryna Piontkivska for the assistance in creating graphs in the R language. The authors are thankful to Pedro Lamosa for support in the NMR analyses.

■ REFERENCES

(1) Geyer, R.; Jambeck, J. R.; Law, K. L. Production, Use, and Fate of All Plastics Ever Made - Supplementary Information. *Sci. Adv.* **2017**, *3*, 25−29.

(2) Brockhaus, S.; Petersen, M.; Kersten, W. A Crossroads for Bioplastics: Exploring Product Developers' Challenges to Move beyond Petroleum-Based Plastics. *J. Cleaner Prod.* **2016**, *127*, 84−95.
(3) Karan, H.; Funk, C.; Grabert, M.; Oey, M.; Hankamer, B. Green Bioplastics as Part of a Circular Bioeconomy. *Trends Plant Sci.* **2019**, *24*, 237−249.
(4) Heredia-Guerrero, J. A.; Heredia, A.; Domínguez, E.; Cingolani, R.; Bayer, I. S.; Athanassiou, A.; Benítez, J. J. Cutin from Agro-Waste as a Raw Material for the Production of Bioplastics. *J. Exp. Bot.* **2017**, *68*, 5401−5410.
(5) Zhang, B. X.; Uyama, H. Biomimic Plant Cuticle from Hyperbranched Poly(Ricinoleic Acid) and Cellulose Film. *ACS Sustainable Chem. Eng.* **2016**, *4*, 363−369.
(6) Domínguez, E.; Heredia-Guerrero, J. A.; Heredia, A. Plant Cutin Genesis: Unanswered Questions. *Trends Plant Sci.* **2015**, *20*, 551−558.
(7) Kolattukudy, P. E. Cutin from Plants. *Biopolym. Online* **2005**, 1−12.
(8) Fich, E. A.; Segerson, N. A.; Rose, J. K. C. The Plant Polyester Cutin: Biosynthesis, Structure, and Biological Roles. *Annu. Rev. Plant Biol.* **2016**, *67*, 207−233.
(9) Domínguez, E.; Heredia-Guerrero, J. A.; Heredia, A. The Plant Cuticle: Old Challenges, New Perspectives. *J. Exp. Bot.* **2017**, *68*, 5251−5255.
(10) Joubès, J.; Domergue, F.Biosynthesis of the Plant Cuticle. In *Hydrocarbons, Oils and Lipids: Diversity, Origin, Chemistry and Fate*, Springer, 2018; pp 1−19.
(11) Yeats, T. H.; Rose, J. K. C. The Formation and Function of Plant Cuticles. *Plant Physiol.* **2013**, *163*, 5−20.
(12) Heredia-Guerrero, J. A.; Guzman-Puyol, S.; Benítez, J. J.; Athanassiou, A.; Heredia, A.; Domínguez, E. Plant Cuticle under Global Change: Biophysical Implications. *Global Change Biol.* **2018**, *24*, 2749−2751.
(13) Bedoić, R.; Ćosić, B.; Duić, N. Technical Potential and Geographic Distribution of Agricultural Residues, Co-Products and by-Products in the European Union. *Sci. Total Environ.* **2019**, *686*, 568−579.
(14) *The Tomato Market in the EU: Volume 1: Production and Area Statistics*; European Commission, 2021.
(15) Benítez, J. J.; Castillo, P. M.; del Río, J. C.; León-Camacho, M.; Domínguez, E.; Heredia, A.; Guzmán-Puyol, S.; Athanassiou, A.; Heredia-Guerrero, J. A. Valorization of Tomato Processing By-Products: Fatty Acid Extraction and Production of Bio-Based Materials. *Materials* **2018**, *11*, 2211.
(16) Mouden, S.; Kappers, I. F.; Klinkhamer, P. G. L.; Leiss, K. A. Cultivar Variation in Tomato Seed Coat Permeability Is an Important Determinant of Jasmonic Acid Elicited Defenses Against Western Flower Thrips. *Front. Plant Sci.* **2020**, *11*, No. 576505.
(17) Marc, M.; Risani, R.; Desnoes, E.; Falourd, X.; Pontoire, B.; Rodrigues, R.; Escórcio, R.; Batista, A. P.; Valentin, R.; Gontard, N.; Silva Pereira, C.; Lopez, C.; Leroy, E.; Lourdin, D.; Marion, D.; Bakan, B. Bioinspired Co-Polyesters of Hydroxy-Fatty Acids Extracted from Tomato Peel Agro-Wastes and Glycerol with Tunable Mechanical, Thermal and Barrier Properties. *Ind. Crops Prod.* **2021**, *170*, No. 113718.
(18) Philippe, G.; Gaillard, C.; Petit, J.; Geneix, N.; Dalgalarrondo, M.; Bres, C.; Mauxion, J. P.; Franke, R.; Rothan, C.; Schreiber, L.; Marion, D.; Bakan, B. Ester Cross-Link Profiling of the Cutin Polymer of Wild-Type and Cutin Synthase Tomato Mutants Highlights Different Mechanisms of Polymerization. *Plant Physiol.* **2016**, *170*, 807−820.
(19) Tedeschi, G.; Benitez, J. J.; Ceseracciu, L.; Dastmalchi, K.; Itin, B.; Stark, R. E.; Heredia, A.; Athanassiou, A.; Heredia-Guerrero, J. A. Sustainable Fabrication of Plant Cuticle-Like Packaging Films from Tomato Pomace Agro-Waste, Beeswax, and Alginate. *ACS Sustainable Chem. Eng.* **2018**, *6*, 14955−14966.
(20) Al-Wandawi, H.; Abdul-Rahman, M.; Al-Shaikhly, K. Tomato Processing Wastes as Essential Raw Materials Source. *J. Agric. Food Chem.* **1985**, *33*, 804−807.
(21) Tedeschi, G.; Benitez, J. J.; Ceseracciu, L.; Dastmalchi, K.; Itin, B.; Stark, R. E.; Heredia, A.; Athanassiou, A.; Heredia-Guerrero, J. A. Sustainable Fabrication of Plant Cuticle-Like Packaging Films from Tomato Pomace Agro-Waste, Beeswax, and Alginate. *ACS Sustainable Chem. Eng.* **2018**, *6*, 14955−14966.
(22) Moreira, C. J.; Bento, A.; Pais, J.; Petit, J.; Escórcio, R.; Correia, V.; Pinheiro, Â.; Haliński, ŁP.; Mykhaylyk, O. O.; Rothan, C.; Silva Pereira, C. An Ionic Liquid Extraction That Preserves the Molecular Structure of Cutin Shown by Nuclear Magnetic Resonance. *Plant Physiol.* **2020**, *184*, 592.
(23) Chatterjee, S.; Sarkar, S.; Oktawiec, J.; Mao, Z.; Niitsoo, O.; Stark, R. E. Isolation and Biophysical Study of Fruit Cuticles. *J. Visualized Exp.* **2012**, 1−7.
(24) Petracek, P. D.; Bukovac, M. J. Rheological Properties of Enzymatically Isolated Tomato Fruit Cuticle. *Plant Physiol.* **1995**, *109*, 675−679.
(25) Round, A. N.; Van, B.; Dang, S.; Estephan, R.; Stark, R. E.; Batteas, J. D. The Influence of Water on the Nanomechanical Behavior of the Plant Biopolyester Cutin as Studied by AFM and Solid-State NMR. *Biophys. J.* **2000**, *79*, 2761−2767.
(26) Pacchiano, R. A.; Sohn, W.; Chlanda, V. L.; Garbow, J. R.; Stark, R. E. Isolation and Spectral Characterization of Plant-Cuticle Polyesters. *J. Agric. Food Chem.* **1993**, *41*, 78−83.
(27) Isaacson, T.; Kosma, D. K.; Matas, A. J.; Buda, G. J.; He, Y.; Yu, B.; Pravitasari, A.; Batteas, J. D.; Stark, R. E.; Jenks, M. A.; Rose, J. K. C. Cutin Deficiency in the Tomato Fruit Cuticle Consistently Affects Resistance to Microbial Infection and Biomechanical Properties, but Not Transpirational Water Loss. *Plant J.* **2009**, *60*, 363−377.
(28) Bento, A.; Moreira, C. J. S.; Correia, V. G.; Escórcio, R.; Rodrigues, R.; Tomé, A. S.; Geneix, N.; Petit, J.; Bakan, B.; Rothan, C.; Mykhaylyk, O. O.; Pereira, C. S. Quantification of Structure−Property Relationships for Plant Polyesters Reveals Suberin and Cutin Idiosyncrasies. *ACS Sustainable Chem. Eng.* **2021**, *9*, 15780−15792.
(29) Correia, V. G.; Bento, A.; Pais, J.; Rodrigues, R.; Haliński, P.; Frydrych, M.; Greenhalgh, A.; Stepnowski, P.; Vollrath, F.; King, A. W. T.; Pereira, C. S. The Molecular Structure and Multifunctionality of the Cryptic Plant Polymer Suberin. *Mater. Today Bio* **2020**, *5*, No. 100039.
(30) Garcia, H.; Ferreira, R.; Martins, C.; Sousa, A. F.; Freire, C. S. R.; Silvestre, A. J. D.; Kunz, W.; Rebelo, L. P. N.; Silva Pereira, C. Ex Situ Reconstitution of the Plant Biopolyester Suberin as a Film. *Biomacromolecules* **2014**, *15*, 1806−1813.
(31) Petkovic, M.; Ferguson, J. L.; Gunaratne, H. Q. N.; Ferreira, R.; Leitão, M. C.; Seddon, K. R.; Rebelo, L. P. N.; Pereira, C. S. Novel Biocompatible Cholinium-Based Ionic Liquids - Toxicity and Biodegradability. *Green Chem.* **2010**, *12*, 643−649.
(32) Meng, X.; Crestini, C.; Ben, H.; Hao, N.; Pu, Y.; Ragauskas, A. J.; Argyropoulos, D. S. Determination of Hydroxyl Groups in Biorefinery Resources via Quantitative 31P NMR Spectroscopy. *Nat. Protoc.* **2019**, *14*, 2627−2647.
(33) Graça, J.; Lamosa, P. Linear and Branched Poly(ω-Hydroxyacid) Esters in Plant Cutins. *J. Agric. Food Chem.* **2010**, *58*, 9666−9674.
(34) Yuan, T. Q.; Sun, S. N.; Xu, F.; Sun, R. C. Characterization of Lignin Structures and Lignin-Carbohydrate Complex (LCC) Linkages by Quantitative 13C and 2D HSQC NMR Spectroscopy. *J. Agric. Food Chem.* **2011**, *59*, 10604−10614.
(35) Balakshin, M.; Capanema, E. A.; Chen, C.-L.; Gracz, H. S. Elucidation of the Structures of Residual and Dissolved Pine Kraft Lignins Using an HMQC NMR Technique Elucidation of the Structures of Residual and Dissolved Pine Kraft Lignins Using an HMQC NMR Technique. *J. Agric. Food Chem.* **2003**, *51*, 6116−6127.
(36) Chu, S.; Subrahmanyam, A. V.; Huber, G. W. The Pyrolysis Chemistry of a β-O-4 Type Oligomeric Lignin Model Compound. *Green Chem.* **2013**, *15*, 125−136.
(37) Mounet, F.; Lemaire-Chamley, M.; Maucourt, M.; Cabasson, C.; Giraudel, J. L.; Deborde, C.; Lessire, R.; Gallusci, P.; Bertrand, A.; Gaudillère, M.; Rothan, C.; Rolin, D.; Moing, A. Quantitative Metabolic Profiles of Tomato Flesh and Seeds during Fruit

Development: Complementary Analysis with ANN and PCA. *Metabolomics* **2007**, *3*, 273−288.
(38) Kumar, M.; Tomar, M.; Bhuyan, D. J.; Punia, S.; Grasso, S.; Sá, A. G. A.; Carciofi, B. A. M.; Arrutia, F.; Changan, S.; Radha; Singh, S.; Dhumal, S.; Senapathy, M.; Satankar, V.; Anitha, T.; Sharma, A.; Pandiselvam, R.; Amarowicz, R.; Mekhemar, M. Tomato (Solanum Lycopersicum L.) Seed: A Review on Bioactives and Biomedical Activities. *Biomed. Pharmacother.* **2021**, *142*, No. 112018.
(39) Petró-Turza, M. Flavor of Tomato and Tomato Products. *Food Rev. Int.* **2009**, *2*, 309−351.
(40) Chung, T. Y.; Hayase, F.; Kato, H. Volatile Components of Ripe Tomatoes and Their Juices, Purées and Pastes. *Agric. Biol. Chem.* **1983**, *47*, 343−351.
(41) Zeisler-Diehl, V. V.; Barthlott, W.; Schreiber, L.Plant Cuticular Waxes: Composition, Function, and Interactions with Microorganisms. In *Hydrocarbons, Oils and Lipids: Diversity, Origin, Chemistry and Fate*, Springer, 2020; pp 123−138.
(42) Balakshin, M.; Capanema, E. A.; Chen, C.-L.; Gracz, H. S. Elucidation of the Structures of Residual and Dissolved Pine Kraft Lignins Using an HMQC NMR Technique Elucidation of the Structures of Residual and Dissolved Pine Kraft Lignins Using an HMQC NMR Technique. *J. Agric. Food Chem.* **2003**, *51*, 6116−6127.
(43) Kosma, D. K.; Parsons, E. P.; Isaacson, T.; Lü, S.; Rose, J. K. C.; Jenks, M. A. Fruit Cuticle Lipid Composition during Development in Tomato Ripening Mutants. *Physiol. Plant* **2010**, *139*, 107−117.
(44) Fernandez-Moreno, J. P.; Levy-Samoha, D.; Malitsky, S.; Monforte, A. J.; Orzaez, D.; Aharoni, A.; Granell, A. Uncovering Tomato Quantitative Trait Loci and Candidate Genes for Fruit Cuticular Lipid Composition Using the Solanum Pennellii Introgression Line Population. *J. Exp. Bot.* **2017**, *68*, 2703−2716.
(45) Romero, P.; Rose, J. K. C. A Relationship between Tomato Fruit Softening, Cuticle Properties and Water Availability. *Food Chem.* **2019**, *295*, 300−310.
(46) Casillas-Vargas, G.; Ocasio-Malavé, C.; Medina, S.; Morales-Guzmán, C.; del Valle, R. G.; Carballeira, N. M.; Sanabria-Ríos, D. J. Antibacterial Fatty Acids: An Update of Possible Mechanisms of Action and Implications in the Development of the next-Generation of Antibacterial Agents. *Prog. Lipid Res.* **2021**, *82*, No. 101093.
(47) Yoon, B. K.; Jackman, J. A.; Valle-González, E. R.; Cho, N. J. Antibacterial Free Fatty Acids and Monoglycerides: Biological Activities, Experimental Testing, and Therapeutic Applications. *Int. J. Mol. Sci.* **2018**, *19*, 1114.
(48) Zheng, C. J.; Yoo, J. S.; Lee, T. G.; Cho, H. Y.; Kim, Y. H.; Kim, W. G. Fatty Acid Synthesis Is a Target for Antibacterial Activity of Unsaturated Fatty Acids. *FEBS Lett.* **2005**, *579*, 5157−5162.
(49) Guzman, J. D. Natural Cinnamic Acids, Synthetic Derivatives and Hybrids with Antimicrobial Activity. *Molecules* **2014**, *19*, 19292−19349.
(50) Kozłowska, J.; Grela, E.; Baczynska, D.; Grabowiecka, A.; Anioł, M. Novel O-Alkyl Derivatives of Naringenin and Their Oximes with Antimicrobial and Anticancer Activity. *Molecules* **2019**, *24*, 679.
(51) Lindner, N.; Casey, J. Unsaturated Aliphatic Dicarboxylic Acids. European Patent EP0662946B1, 1998.
(52) Osman, S. F.; Irwin, P.; Fett, W. F.; O'Connor, J. V.; Parris, N. Preparation, Isolation, and Characterization of Cutin Monomers and Oligomers from Tomato Peels. *J. Agric. Food Chem.* **1999**, *47*, 799−802.
(53) Meng, X.; Crestini, C.; Ben, H.; Hao, N.; Pu, Y.; Ragauskas, A. J.; Argyropoulos, D. S. Determination of Hydroxyl Groups in Biorefinery Resources via Quantitative 31P NMR Spectroscopy. *Nat. Protoc.* **2019**, *14*, 2627−2647.
(54) Guzman, J. D. Natural Cinnamic Acids, Synthetic Derivatives and Hybrids with Antimicrobial Activity. *Molecules* **2014**, *19*, 19292−19349.
(55) Kozłowska, J.; Grela, E.; Baczynska, D.; Grabowiecka, A.; Anioł, M. Novel O-Alkyl Derivatives of Naringenin and Their Oximes with Antimicrobial and Anticancer Activity. *Molecules* **2019**, *24*, 679.
(56) Chang, S. T.; Chen, P. F.; Chang, S. C. Antibacterial Activity of Leaf Essential Oils and Their Constituents from Cinnamomum Osmophloeum. *J. Ethnopharmacol.* **2001**, *77*, 123−127.
(57) Blaskovich, M. A. T.; Elliott, A. G.; Kavanagh, A. M.; Ramu, S.; Cooper, M. A. In Vitro Antimicrobial Activity of Acne Drugs Against Skin-Associated Bacteria. *Sci. Rep.* **2019**, *9*, No. 14658.
(58) Zlotnik-Mazori, T.; Stark, R. E. Nuclear Magnetic Resonance Studies of Cutin, an Insoluble Plant Polyester. *Macromolecules* **1988**, *21*, 2412−2417.
(59) Bhunia, R. K.; Showman, L. J.; Jose, A.; Nikolau, B. J. Combined Use of Cutinase and High-Resolution Mass-Spectrometry to Query the Molecular Architecture of Cutin. *Plant Methods* **2018**, *14*, 117.
(60) Ferreira, R.; Garcia, H.; Sousa, A. F.; Petkovic, M.; Lamosa, P.; Freire, C. S. R.; Silvestre, A. J. D.; Rebelo, L. P. N.; Pereira, C. S. Suberin Isolation from Cork Using Ionic Liquids: Characterisation of Ensuing Products. *New J. Chem.* **2012**, *36*, 2014−2024.
(61) Dołżonek, J.; Kowalska, D.; Maculewicz, J.; Stepnowski, P.Regeneration, Recovery, and Removal of Ionic Liquids. In *Encyclopedia of Ionic Liquids*, Springer, 2020; pp 1−9.
(62) Dotsenko, A. S.; Denisenko, Y. A.; Rozhkova, A. M.; Zorov, I. N.; Shashkov, I. A. Implementation of Microfiltration in Recycled Usage of Ionic Liquid BmimCl and Deep Eutectic Solvent ChCl/Acetic Acid for Lignocellulosic Biomass Conversion. *Bioresour. Technol. Rep.* **2022**, *17*, No. 100887.

https://doi.org/10.1021/acssuschemeng.2c03437
ACS Sustainable Chem. Eng. 2022, 10, 11415−11427